ARTICLE

Dioxythiophene-Based Polymer Electrodes for Supercapacitor Modules

David Y. Liu and John R. Reynolds*

The George and Josephine Butler Polymer Research Laboratory; Department of Chemistry and Center for Macromolecular Science and Engineering; University of Florida, Gainesville, Florida 32611-7200, United States

ABSTRACT We report on the electrochemical and capacitive behaviors of poly(2,2-dimethyl-3,4-propylene-dioxythipohene) (PProDOT-Me_2) films as polymeric electrodes in Type I electrochemical supercapacitors. The supercapacitor device displays robust capacitive charging/discharging behaviors with specific capacitance of 55 F/g, based on 60 μg of PProDOT-Me_2 per electrode, that retains over 85% of its storage capacity after 32 000 redox cycles at 78% depth of discharge. Moreover, an appreciable average energy density of 6 Wh/kg has been calculated for the device, along with well-behaved and rapid capacitive responses to 1.0 V between 5 to 500 mV s^{-1}. Tandem electrochemical supercapacitors were assembled in series, in parallel, and in combinations of the two to widen the operating voltage window and to increase the capacitive currents. Four supercapacitors coupled in series exhibited a 4.0 V charging/discharging window, whereas assembly in parallel displayed a 4-fold increase in capacitance. Combinations of both serial and parallel assembly with six supercapacitors resulted in the extension of voltage to 3 V and a 2-fold increase in capacitive currents. Utilization of bipolar electrodes facilitated the encapsulation of tandem supercapacitors as individual, flexible, and lightweight supercapacitor modules.

KEYWORDS: electroactive conjugated polymer • 3,4-propylenedioxythiophene • energy storage • tandem supercapacitor

INTRODUCTION

Electroactive conjugated polymers (ECPs) have shown substantial promise in applications of organic devices from energy harvesting (1) to electrochromic displays (2). One of the emerging fields of conjugated polymer research is in the development of electrode materials in charge storing applications (3−5). The perspective of manufacturing low-cost, lightweight, and flexible power storage devices for applications such as portable consumer electronics, military applications, and electronic vehicles has motivated this field of research to the forefront.

Electrochemical supercapacitors of relatively high energy and power densities are part of a significant field of electrochemical energy storage as they bridge the gap between conventional capacitors and batteries (4, 6). Specifically, electroactive polymers are attractive capacitive materials as they are capable of storing charge in the electrical double layer, as well as in the polymer matrix by rapid faradaic charge transfer. The redox process requires an intimate interaction between polymer films and the electrolytes for ions to not only penetrate though the polymeric matrix, but also to maintain electroneutrality of the system, which ultimately gives rise to charge storage responses (3, 7).

In addition to conducting polymers as charge storing electrodes, other types of energy storage materials in supercapacitors include carbon composites and inorganic metal oxides. Contrary to redox-active supercapacitors, carbon-based double layer capacitors operate solely on electrostatic surface charge accumulation. Inorganic materials, such as ruthenium oxides and other metal oxides, have also shown promise, but these materials typically suffer from poor electrical conductivity. In contrast, conjugated polymers have high conductivity in their doped state and display fast, reversible, and stable electrochemical behavior. Redox-active supercapacitors can be designed to ensure that the entire volume of the polymer is involved in the charge storage process. Furthermore, there is great potential in utilizing ECPs for charge storage devices as these polymer materials exhibit reduced cost, weight, and environmental impact relative to the traditional inorganic materials.

While highly regarded as the first conducting polymer discovered by MacDiarmid et al., polyacetylene also functioned as the prototype material in polymeric charge storage applications (8−10). Polyacetylene electrodes have the ability to constitute as both the cathode and the anode with p-doping and n-doping capabilities; however, the advancement of polyacetylene-based batteries was hindered because of inherent instability and processing difficulties. Although polyacetylene set the platform for ECP-based batteries, the ability to utilize capacitive currents of electroactive conducting polymers was later suggested by Feldberg in his electrochemical analyses of polypyrrole and polythiophene (11).

Since the initial reports of utilizing electroactive polymers in redox-active supercapacitors (7, 12, 13), there has been continuous interest in developing other conjugated polymers in charge storing applications, in particular polyaniline, polypyrrole, polythiophene, and their derivatives (14−19). Polyaniline has demonstrated charging storing capabilities in both nonaqueous and aqueous electrolytes with high electrochemical stabilities and specific capacitances ranging from 100 to 250 F/g (20). Polypyrrole has also shown

* To whom correspondence should be addressed. E-mail: reynolds@chem.ufl.edu.

Received for review August 21, 2010 and accepted October 29, 2010

DOI: 10.1021/am1007744

Published on Web 11/22/2010

promise in both battery and supercapacitor research with specific capacitance of 40−85 F/g (12, 21, 22). Polythiophene, albeit with reports of high capacitance values of 250 F/g, has shown limited progress in energy storage because of their electrochemical instability (23). However, electron-rich derivatives of polythiophene, for example, poly(3,4-ethylenedioxythiophene) (PEDOT), have been extensively studied as a supercapacitor electrode because of their excellent electrochemical stability, fast redox switching speeds and high specific capacitances (24−26).

Subsequently, derivatives of poly(3,4-alkylenedioxythiophene)s that are structurally similar to PEDOT have been developed for electrochemical devices. Chemically synthesized poly(3,4-propylenedioxythiophene) (PProDOT) and similar derivatives have been well-characterized as electrochromic polymers due to their high optical contrast, rapid switching times, electrochemical lifetimes, and high coloration efficiency (27−29). Although PProDOTs exhibit excellent electrochromic properties, their capacitive behavior has not received as extensive attention. Previously, Stenger-Smith prepared Type II supercapacitors based on two different p-dopable electron-rich conjugated polymers, PEDOT and PProDOT, in which capacitive properties were investigated as a function of supporting electrolytes (30). Their results showed improved electrochemical stability in ionic liquid electrolytes, specifically, 1-ethyl-3-methyl-1*H*-imidazolium bis(trifluoromethanesulfonyl)imide (EMI-BTI). Also, Schulz demonstrated capacitive behavior of PProDOT films on carbon fiber microelectrodes as charge storing materials (31). Most recently, Irvin investigated PProDOT-based supercapacitors utilizing ionic liquid electrolyte blends at low temperatures from −30 °C up to 60 °C, with 10% capacity loss after 10 000 cycles at 70% depth of discharge (32).

In this report, we describe the electrochemical polymerization and capacitive properties of PProDOT-Me_2 as polymeric electrodes for Type I electrochemical supercapacitors. Exhibiting excellent capacitive behavior between −0.7 to 0.8 V versus Ag/Ag^+, rapid redox switching from 10 to 1000 mVs^{-1}, and stable electrochemical responses, films of PProDOT-Me_2 are excellent charge storing materials for ECP-based supercapacitors. As such, constructed with PProDOT-Me_2 electrodes, Type I electrochemical supercapacitors display robust capacitive currents within a 1.0 V window, rapid redox switching up to 500 mVs^{-1}, and a stable electrochemical switching lifetime of over 32 000 cycles at 100 mVs^{-1} and 78% depth of discharge. These results are comparable to the Type II supercapacitors based on the parent PEDOT and PProDOT mentioned above (30) and position us well for developing these capacitors further. In addition, we describe our abilities to extend the cell voltage and capacitive currents with multiple supercapacitors coupled in tandem. To date, there has been little reported effort in developing electroactive polymer based supercapacitor modules and, to the best of our knowledge, no previous report of compact laminated devices (33). In our work, a stable 4.0 V tandem device was assembled with four supercapacitors in series, whereas a 4-fold increase in capacitive currents was obtained with parallel constructs. The potential of a tandem supercapacitor is realized in the combination of both serial and parallel assemblies to achieve high cell voltage and capacity simultaneously. These studies demonstrate the ability to couple supercapacitors, which with the use of bipolar electrodes, are ultimately encapsulated as a single supercapacitor module.

EXPERIMENTAL SECTION

Materials. 2,2-Dimethyl-3,4-propylenedioxythiophene (ProDOT-Me_2) was synthesized via the transetherification between 3,4-dimethoxythiophene and 2,2-dimethyl-1,3-propanediol according to the methodologies previously reported (34). 1-Ethyl-3-methyl-1-*H*-imidazolium bis(trifluoromethylsulfonyl) imide (EMI-BTI) was purchased from Covalent Associates Inc. and lithium bis-(trifluoromethylsulfonyl)imide (Li-BTI) was purchased from Aldrich and both were used as received. Propylene carbonate (PC) and acetonitrile (ACN), purchased from Sigma-Aldrich, were distilled over calcium hydride prior to use. Gold-coated Kapton substrates (Gold 1000 Å; 1 mil Kapton/3 M 966 adhesive) were purchased from Astral Technology Unlimited. Contacts for the electrodes were made from conductive adhesive copper tape (1131, 3M). Thermal encapsulation lamination (Wilson Jones, LP35HS) was utilized with heat seal laminating pouch (GBC, 3 mil).

Electrode Formation and Characterization. All electrochemistry was performed using an EG&G model PAR273A potentiostat/galvanostat. ProDOT-Me_2 was electrochemically polymerized and deposited by potentiodynamic deposition scans in a three-electrode cell containing 10 mM ProDOT-Me_2 in 0.1 M LiBTI/acetonitrile supporting electrolyte. The extent of electrodeposition was controlled by the number of potentiodynamic deposition scans (e.g., five deposition scans corresponds to approximately 25 mC/cm^2 of charge) between −1.0 to 1.31 V versus Ag/Ag^+ at 50 mVs^{-1}. The area of gold/Kapton electrode coated with polymer is predetermined by the surface area immersed in the electrochemical cell, in this case ∼1.0 cm^2. Electrodeposition and electrochemical studies of the polymer films were carried out in a single-compartment three-electrode cell with a platinum flag as the counter electrode, Ag/Ag^+ as the reference electrode containing 10 mM $AgNO_3$ in 0.1 M LiBTI/ACN supporting electrolyte solution, and gold/Kapton as the working electrodes. Bipolar electrode were prepared by adhering two gold/Kapton electrodes between an insulator. Electrochemical polymerization onto bipolar electrodes proceeds via a "pseudo flat-cell" in which the gold/Kapton as the working electrode is localized between single-compartment three-electrode cells. The bipolar electrodes are reinforced with copper tape on the side of electrodeposition to ensure no electrical shorting occurred.

Assembly of Supercapacitor Device. PProDOT-Me_2 was electrochemically polymerized using the previously discussed methods. Flexible conductive gold-coated Kapton electrode substrate (∼1.0 × 2.0 cm^2) was used as the working electrode. Electrochemically deposited polymer films covered the gold-coated Kapton (∼1.0 cm^2), leaving ∼1.0 cm^2 free of polymer. The working electrode (cathode) was oxidatively doped (0.9 V versus Ag/Ag^+ for 30 s), while the counter electrode (anode) was neutralized (−0.6 V versus Ag/Ag^+ for 30 s) prior to device assembly to ensure balance of charge. Ionic liquid electrolyte blend (1:1 ratio of EMI-BTI to PC) was applied to the polymer surface before encapsulation. A 30 μM thick separator paper was placed between the two electrodes. The device was thermally encapsulated with 3 mil laminate pouch. All device fabrications and electrochemical measurements were performed in air.

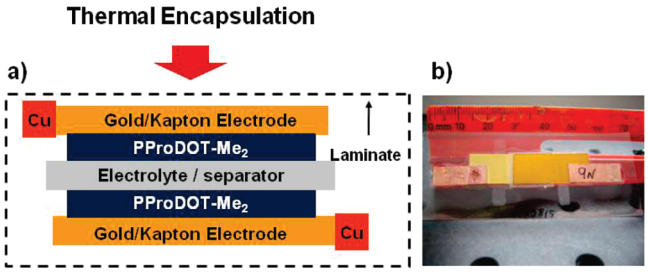

FIGURE 1. (a) Schematic and (b) photograph of a thermally laminated Type I PProDOT-Me_2 based electrochemical supercapacitor.

RESULTS AND DISCUSSION

Polymer-Based Supercapacitors. A schematic diagram for the electrochemical supercapacitor device utilizing PProDOT-Me_2 characterized in this study is shown in Figure 1. The general assembly method for these supercapacitor devices employ a sandwich-type configuration of two facing conductive electrodes coated with electropolymerized electroactive polymers and separated by a porous membrane containing ionically conductive electrolyte. The use of another PProDOT-Me_2 as the counter electrode ensures charge balance of redox reactions taking place on the cathode and the anode during the charging and discharging processes. In scenarios of supercapacitor modules, as elaborated in later sections, bipolar electrodes are utilized with multiple cathodes and anodes sandwiched to construct the module device. In this report, symmetrical electrodes are the focus in developing highly capacitive, rapid redox switching, large cell voltage, and highly stable Type I PProDOT-Me_2-based supercapacitors.

Polymer Electrode Properties. Figure 2a shows a repeated oxidative cyclic voltammetric electropolymerization of PProDOT-Me_2 on a gold/Kapton substrate. The gold on Kapton provides high conductivity and excellent mechanical flexibility. The initial anodic sweep displays a monomer oxidation peak potential ($E_{p,m}$) of 1.21 V vs Ag/Ag^+. Subsequent scans exhibit increases in current density (between −0.5 V to 1.0 V vs Ag/Ag^+), which is indicative of electrodeposition on the working electrode. The resulting polymer is electrochemically cycled in monomer-free supporting electrolyte, demonstrating a highly reproducible redox (doping/undoping) process centered at −0.31 V ($E_{1/2}$), which is determined from the average of the peak anodic potential (−0.23 V) and the peak cathodic potential (−0.39 V) (Figure 2b). The amount of electrodeposited polymer on the electrode was controlled by the number of potentiodynamic cycles during electropolymerization. It is necessary to have the same amount of polymer on each electrode to maintain charge balance upon charging and discharging in the supercapacitor device.

The polymer electrochemistry is monitored as a function of increasing scan rates (10 to 1000 mV s^{-1}) in Figure 2c in which the peak currents are probed as a function of scan rate (Figure 2d). The linear dependence indicates the redox process is electrode-confined and well-behaved to relatively rapid switching rates. Prior to supercapacitor assembly, polymer films are neutralized and oxidized at constant potentials (−0.6 and 0.9 V vs Ag/Ag^+) to prepare the anode and cathode.

Type I Supercapacitor. The charging/discharging cyclic voltammogram of a Type I PProDOT-Me_2 based supercapacitor as a two-electrode cell is highlighted in Figure 3a. The supercapacitor demonstrates near ideal and highly

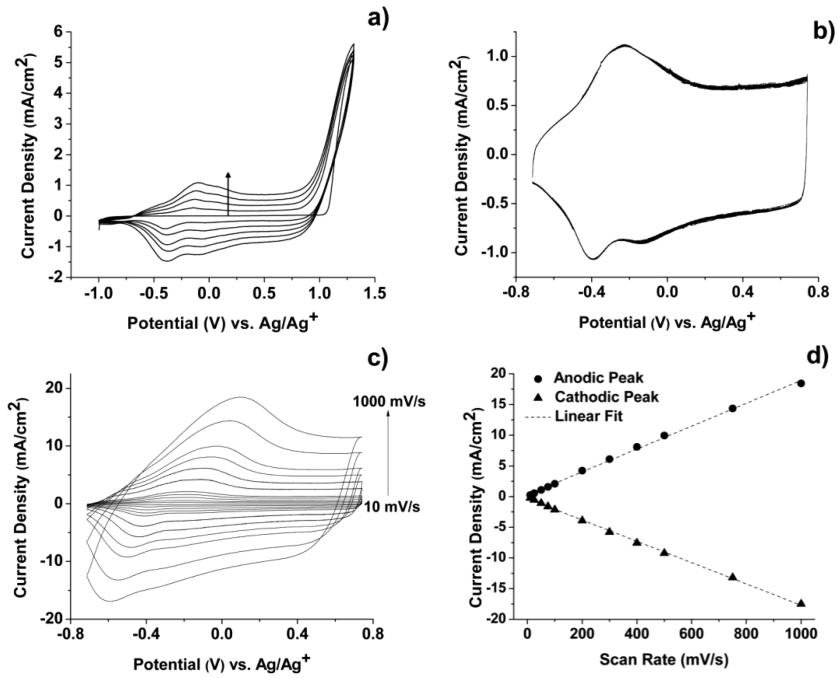

FIGURE 2. (a) Electrodeposition of PProDOT-Me_2 on Au/Kapton substrates via 5 repetitive potentiodynamic cycles from −1.0 to +1.31 V vs Ag/Ag^+ at 50 mVs^{-1} using 10 mM ProDOT-Me_2 in 0.1 M LiBTI/ACN supporting electrolyte (b) PProDOT-Me_2 redox switching in 0.1 M LiBTI/ACN supporting electrolyte at 50 mVs^{-1} from −0.7 V to 0.8 V vs Ag/Ag^+ for 20 cycles (approximately 25 mC/cm^2 of charge). (c) Electrochemical redox switching of PProDOT-Me_2 as a function of increasing scan rates, from 10 to 1000 mV s^{-1}. (d) Anodic and cathodic peak current as a function of scan rate showing linear dependence.

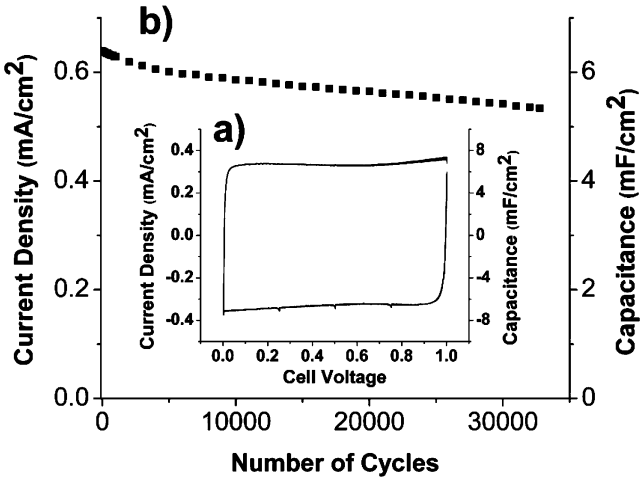

FIGURE 3. (a) Two-electrode device with symmetric PProDOT-Me_2 electrodes. Device charging and discharging at 50 mVs^{-1} at 1.0 V voltage window. (b) Device current density and capacitance for a separate device at 0.5 V, with 85% capacity retained over 32 000 charging/discharging cycles at 100 mVs^{-1}.

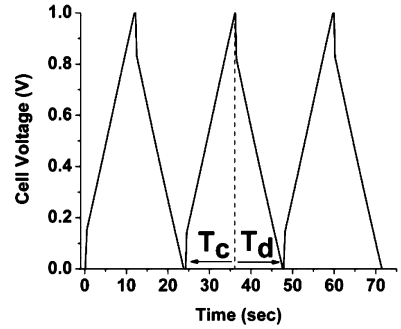

FIGURE 5. Galvanic charging/discharging curves of a single symmetric PProDOT-Me_2 supercapacitor. Potentials were cycled from 0.0 to 1.0 V at a current density of 0.5 mA/cm^2. T_c and T_d represent charge and discharge time, respectively.

capacitive response as observed from the rectangular-shaped CV. As seen from theory in the case of a pure capacitive process, a rapid increase and plateau of current density upon charging followed by its mirror-image upon discharging are distinctive signs of capacitive behavior in these electrochemical capacitor processes. The device maintains stable current (0.3 mA/cm^2) throughout the 1.0 V operating window. The charging/discharging cyclic voltammogram monitored at 50 mVs^{-1} shows minimal current density loss after 50 redox cycles, as the reproducible current response was broken in. It is important to note that the sharp increase and decrease in current density at 0.0 V and 1.0 V respectively demonstrates the ability of the supercapcitor to charge and discharge rapidly. The lifetime of the supercapacitor is monitored with repeated cyclic voltammetric charging and discharging cycles (Figure 3b). After more than 32,000 redox cycles at 78% depth of discharge and 100 mVs^{-1} cycling rate, the supercapacitor retained 85% of its charge storing capacity to demonstrate its ability to perform with high stability requirements.

The ability of the symmetric PProDOT-Me_2 electrochemical supercapacitor to charge and discharge at high scan rates is illustrated in Figure 4a. Scan rate dependence studies between 5 to 500 mVs^{-1} over a 1.0 V operating window demonstrate the supercapacitor to charge and discharge effectively at low and high scanning rates. Even at fast scan rates, the device is capable of maintaining the near ideal rectangular CV shape as excellent capacitive behavior is observed throughout the voltage window at all scan rates with rapid charging and discharging responses. In Figure 4b, a linear relationship is seen between the average current density (monitored at 0.5 V) and the scan rate. This trend indicates the polymeric materials in the device are not only highly electroactive, but the electrolyte in the device effectively compensates both the neutral and oxidized polymer electrodes, especially throughout the entire matrix of the film. More importantly, the supercapacitor areal capacitance is nearly consistent throughout the scan rate regime. This observation is consistent with ideal electrochemical supercapacitors as the capacitance is independent of charging/discharging rates.

To better characterize the behavior of PProDOT-Me_2 for supercapacitor applications, the Type I device was probed under galvanostatic charge/discharge cycles. Figure 5 shows the charging/discharging cycles at an applied constant current of 0.5 mA/cm^2 in the potential range between 0 and +1.0 V. The symmetry of the charge and discharge profile shows good capacitive behavior.

The mirror images of charging and discharging curves demonstrate reproducibility and reversibility, having charging and discharging times of approximately 12 s at 0.5 mA/cm^2 applied currents and as short as 5 s for 1.0 mA/cm^2.

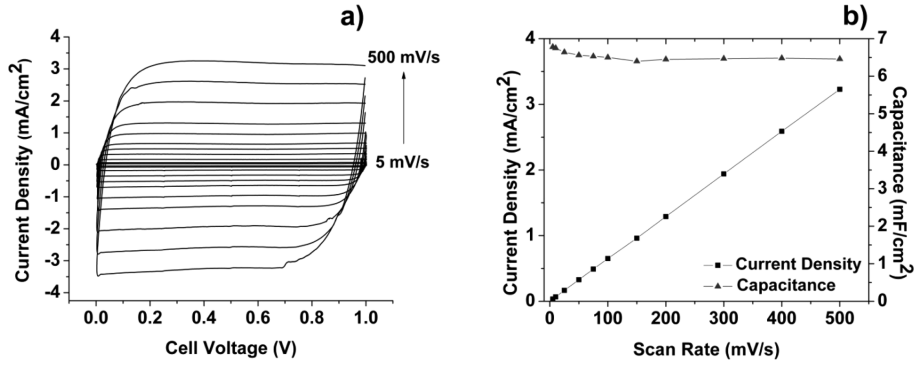

FIGURE 4. (a) Device charging and discharging at as a function of scan rate from 5 to 500 mV s^{-1}. (b) Current and capacitance as a function of scan rate for symmetric PProDOT-Me_2 Type I supercapacitor.

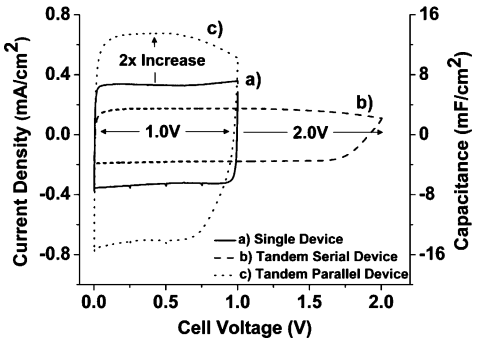

FIGURE 6. Supercapacitor charging/discharging CV at 50 mVs^{-1} for (a) single symmetric PProDOT-Me_2 supercapacitor, (b) two tandem serial supercapacitors, and (c) two tandem parallel supercapacitors. Polymer electrodes prepared via five potentiodynamic electropolymerization cycles ($q = 25$ mC/cm^2).

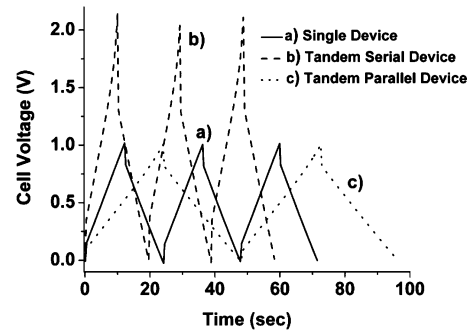

FIGURE 7. Supercapacitor galvanic charging and discharging performances for (a) single supercapacitor, (b) tandem serial supercapacitors, and (c) tandem parallel supercapacitors.

Tandem Supercapacitors. It is well-known that efforts to increase energy density in ECP-based supercapacitors demand not just high, but also a stable operating cell voltage. In this context, n-dopable polymers capable of spanning the cell voltage have previously been developed as charge storing materials (12, 35). While Type III and IV supercapacitors are able to operate in the 2.0−3.0 voltage range, electrochemical instability is often an issue. As a result, there is a trade-off between high energy density and stability at lower voltages. To improve the voltage window without employing n-dopable polymers, we have developed a strategy in which solely p-dopable polymers are utilized and incorporated into supercapacitors coupled in tandem. The assembly of multiple supercapacitors has a cumulative effect in which a widening of cell voltage and an increase in capacitive currents is expected when coupled in series and in parallel, respectively.

As shown via cyclic voltammetry experiments presented in Figure 6, the single supercapacitor (Figure 6a), serving as the model device, shows robust capacitive properties to 1.0 V while passing 0.3 mA/cm^2 of current. With approximately 60 μg of PProDOT-Me_2 and residual electrolyte per electrode, as determined post electrochemical switchings, the specific capacitance relative to total polymer mass is 55 F/g and average energy density of 6 Wh/kg. As two supercapacitors are coupled in series (Figure 6b), the CV exhibits capacitive behavior and reversibility throughout the 2.0 V window with 0.18 mA/cm^2 of current, or 15 F/g relative to the total polymer mass. The ability to maintain a steady current during the charging/discharging processes highlights the capacitive properties of the PProDOT-Me_2 along with the ability to couple supercapacitors successfully. While the tandem serial supercapacitor improves the voltage window, it is important to note the concurrent diminution of current with additional devices. As two supercapacitors are coupled in series, the current is decreased due to added resistance. To address this issue, tandem supercapacitors are assembled in parallel to increase the current passing through. Relative to a single supercapacitor (Figure 6a), the charging/discharging CV of tandem parallel supercapacitors, as illustrated in Figure 6c, exhibits a 2-fold increase in current (55 F/g) while maintaining a steady capacitive behavior and reversibility throughout the 1.0 cell voltage.

Galvanic charging/discharging steps were employed on the tandem supercapacitors to further characterize the behavior of PProDOT-Me_2 for charge storing applications and the ability to couple supercapacitor devices effectively. By applying a constant current of ±0.5 mA/cm^2 to the tandem supercapacitors as a function of time (Figure 7), the galvanic charging-discharging curves highlight the relative charging/discharging times and the operating voltage window. Similar to the CV comparison experiments, the single supercapacitor (Figure 7a) as the model curve, shows 12 s to charge/discharge at 1.0 V. The charging-discharging curves for the tandem serial supercapacitor (Figure 7b) exhibits a 2.0 V window which is in good agreement with the cyclic voltammogram. In contrast, the tandem parallel supercapacitor (Figure 7c) displays 24 s for charging/discharging times to 1.0 V. Here, the times are approximately doubled from that of the single supercapacitor since the applied current passing through the tandem device is shared between two individual devices. While longer charging/discharging times are expected for the tandem supercapacitor in parallel, it allows for opportunities in ride-through power applications where extended charging/discharging times are needed.

The repetitive near-triangular curves emphasize the PProDOT-Me_2 supercapacitor devices are charging and discharging reversibly with similar durations, though the voltage drop suggests internal resistance (Figure 7). A close examination of the galvanic charging/discharging curves shows an ohmic drop, while the cyclic voltammogram (Figure 6) shows an asymmetry in the current response. These observations have been nicely addressed by Bélanger who attributes this behavior to a drop of conductivity in the negative electrode as a result of its nearly undoped state (36). In the case of the Type I supercapacitors discussed here, and perhaps more noticeable in the tandem supercapacitors, our observations are in agreement and consistent with those reported in literature (36, 37). While this is a limitation in electroactive polymer-based supercapacitors, these issues can be circumvented with a lower single-cell voltage (36), as well as proper interfacial contacts within the cell (38).

For the purpose of comparing the effects of multiple tandem supercapacitors, four identical Type I supercapaci-

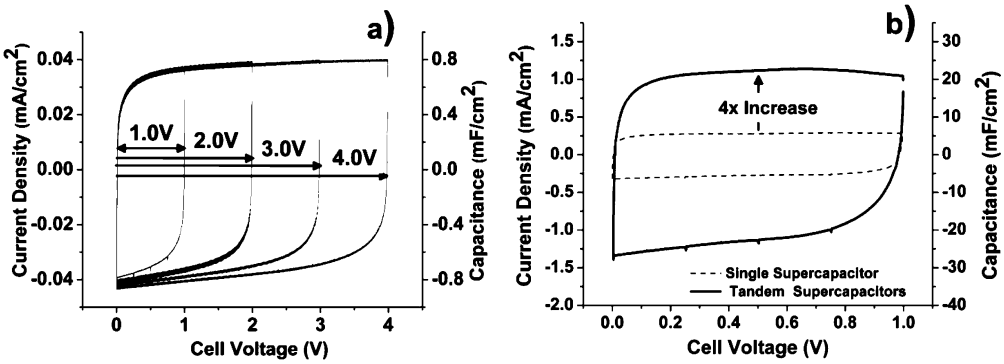

FIGURE 8. (a) Four symmetric PProDOT-Me_2 supercapacitors in series to enhance voltage window from 1.0 to 4.0 V. (b) Four symmetric PProDOT-Me_2 supercapacitors in parallel to increase current by 4-fold.

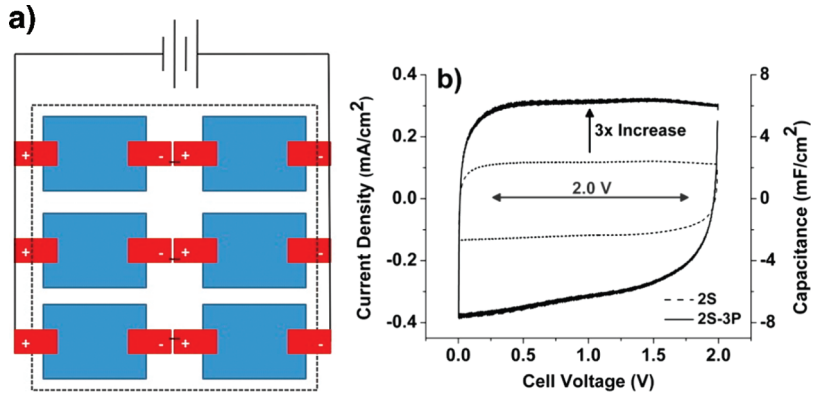

FIGURE 9. (a) Tandem supercapacitor schematic with two devices in series and three sets in parallel (2S-3P) and (b) cyclic voltammograms of 2S-3P.

tors were assembled in series. As illustrated by the cyclic voltammetry profiles in Figure 8a, the tandem serial supercapacitor assembly has an overall cell voltage of 4.0 V. The charging/discharging CVs exhibit high capacitive behavior and reversibility throughout the extended voltage regime. Similarly, the ability to effectively charge/discharge as tandem parallel supercapacitors is demonstrated by the cyclic voltammetry profiles in Figure 8b. The tandem parallel supercapacitor assembly has an overall increase of 4-fold in current density, which is in good agreement with previous supercapacitor devices.

To capitalize on the tandem supercapacitor concept, we connected individual devices both in series and in parallel to extend the cell voltage and increase the capacitance simultaneously. As illustrated in Figure 9a, six identical supercapacitors were integrated with two individual devices connected in series and three sets connected in parallel. With this device organization, we expect the assembly to operate with a 2.0 cell voltage and a 3-fold increase of current density. Figure 9b shows the CV of the six supercapacitor assembly (designated as 2S-3P) superimposed on the response with two supercapacitors in series. The advantage of tandem supercapacitor development allows for design flexibility in voltage and capacitance values. Although not fully optimized in this report, we do not envision a limit to the number of supercapacitor coupled in tandem.

Supercapacitor Module. In our efforts to develop tandem supercapacitors as an individual module that is

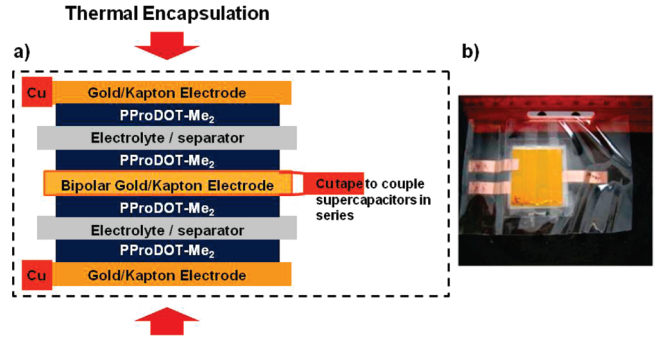

FIGURE 10. Schematic of supercapacitor module employing bipolar electrodes.

stackable and lightweight, bipolar electrodes are utilized as the center component. Weight considerations can benefit from the module architecture as inactive materials, such as inner membranes and packaging materials, are minimized and active materials are maximized. A schematic diagram for the electrochemical supercapacitor module utilizing PProDOT-Me_2 is shown in Figure 10. The general assembly of these modules employs a sandwich-type configuration in which a PProDOT-Me_2 coated bipolar electrode is positioned between two monopolar electrodes to ensure charge balance of the redox species. As such, the electrodes are coupled in series to the exterior electrodes to complete a charged supercapacitor module. The thermal lamination encapsulation of the thin flexible layers nicely compliments in the fabrication of supercapacitor modules as an individual stack.

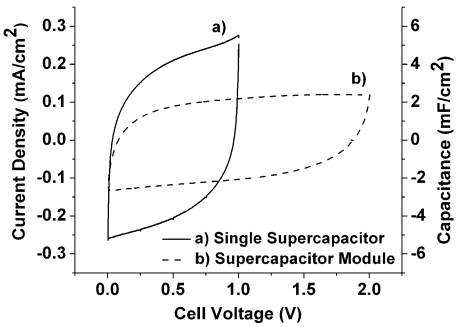

FIGURE 11. Cyclic voltammograms of (a) single supercapacitor and (b) supercapacitor module at 50 mVs^{-1}; Polymer electrodes prepared via three potentiodynamic electropolymerization cycles.

The performance of such a supercapacitor module is illustrated via the cyclic voltammograms in Figure 11. In these experiments, the extent of electrochemical polymerization and deposition of PProDOT-Me$_2$ was maintained to three potentiodynamic scans. As such, the CV of the single supercapacitor device (Figure 11a) displays an average current of 0.2 mA/cm^2 to 1.0 V. In comparison to the supercapacitor module (Figure 11b), the voltage window was successfully extended to 2.0 V and the module exhibits 0.1 mA/cm^2 of capacitive current. The development of supercapacitor modules enables the ability to stack multiple supercapacitors as a single component, although this precludes analyses of individual devices for the possibility of defects.

CONCLUSIONS AND PERSPECTIVES

An electron-rich derivative of dioxythiophene, PProDOT-Me$_2$, was electrochemically polymerized on gold/Kapton substrates to investigate its capacitive properties for charge storage applications in supercapacitors. Redox switching of the PProDOT-Me$_2$ films display stable electrochemical responses between −0.7 to 0.8 V versus Ag/Ag$^+$, while scan rate dependence studies from 10 to 1000 mV s^{-1} suggest the electroactive polymer to be electrode-confined and well-behaved. PProDOT-Me$_2$ was also used to construct polymeric electrodes on gold/Kapton substrates in Type I electrochemical supercapacitors. The supercapacitor devices display robust capacitive behavior over a 1.0 V operating window with scan rates between 5 and 500 mVs^{-1}. The specific capacitance of 55 F/g was calculated based on the active material with average energy density of 6 Wh/kg. Also, the device retains over 85% of its charging/discharging capacity over 32,000 redox cycles at 78% depth of discharge.

As a strategy to improve the voltage window and capacitance of electrochemical supercapacitors, tandem supercapacitors coupled in series and in parallel, and ultimately as a single encapsulated module, were successfully devised and tested. Electrochemical results exhibit the ability to extend the voltage window to 4.0 V and capacitance to 25 mF/cm^2 by the assembly of four tandem supercapacitors in series and in parallel, respectively. The flexibility of supercapacitor design allows for either, or both, voltage and capacitance improvements via serial and parallel constructs to meet the needs of power and energy requirements. Furthermore, development of tandem supercapacitors within a single encapsulation as stackable energy storage devices were successfully fabricated with PProDOT-Me$_2$ on gold/Kapton bipolar electrodes, extending the supercapacitor voltage to 2.0 V.

Ultimately, we envision the electrochemical supercapacitors, while maintaining their flexible and lightweight architecture, as rollable and stackable devices that can supply the power and energy needs in space-limited applications. The ability to process highly capacitive, conjugated electroactive polymers will allow roll-to-roll production of tandem supercapacitors. As such, numerous conducting polymers can be utilized in supercapacitor modules in which highly conductive, electrochemically and mechanically stable electroactive polymers are ideal.

Acknowledgment. The authors gratefully thank the Office of Naval Research, Capacitor Program (N00014-10-1-0454) and ARDEC via Crosslink (W15QKN-07-C-0121) for financial support of this work.

REFERENCES AND NOTES

(1) Thompson, B. C.; Fréchet, J. M. J. *Angew. Chem., Int. Ed.* **2008**, *47*, 58–77.
(2) Beaujuge, P. M.; Reynolds, J. R. *Chem. Rev.* **2010**, *110*, 268–320.
(3) Conway, B. E. *Electrochemical Supercapacitors: Scientific Fundamentals and Technological Applications*; Kluwer Academic/ Plenum: New York, 1999.
(4) Irvin, J. A.; Irvin, D. J.; Stenger-Smith, J. D. Electroactive Polymers for Batteries and Supercapacitors. In *Handbook for Conducting Polymers: Processing and Applications*, 3rd ed.; CRC Press: Boca Raton, FL, 2007; Vol. 1, pp 9/1.
(5) Naoi, K.; Morita, M. *Electrochem. Soc. Interface* **2008**, *17*, 44–47.
(6) Winter, M.; Brodd, R. J. *Chem. Rev.* **2004**, *104*, 4245–4270.
(7) Gottesfeld, S.; Redondo, A.; Feldberg, S. W. *J. Electrochem. Soc.* **1987**, *134*, 271–272.
(8) Kaner, R. B.; MacDiarmid, A. G. *J. Chem. Soc., Faraday Trans.* **1984**, *80*, 2109–2118.
(9) Kaner, R. B.; MacDiarmid, A. G. *Synth. Met.* **1986**, *14*, 3–12.
(10) MacDiarmid, A. G.; Kaner, R. B.; Mammone, R. J.; Heeger, A. J. *J. Electrochem. Soc.* **1981**, *128*, 1651–1654.
(11) Feldberg, S. W. *J. Am. Chem. Soc.* **1984**, *106*, 4671–4674.
(12) Rudge, A.; Davey, J.; Raistrick, I.; Gottesfeld, S.; Ferraris, J. P. *J. Power Sources* **1994**, *47*, 89–107.
(13) Rudge, A.; Raistrick, I.; Gottesfeld, S. *Electrochim. Acta* **1994**, *39*, 273–287.
(14) Carlberg, J. C.; Inganas, O. *J. Electrochem. Soc.* **1997**, *144*, L61–L64.
(15) Fusalba, F.; Belanger, D. *J. Phys. Chem. B* **1999**, *103*, 9044–9054.
(16) Fusalba, F.; El Mehdi, N.; Breau, L.; Belanger, D. *Chem. Mater.* **1999**, *11*, 2743–2753.
(17) Ghosh, S.; Inganas, O. *Adv. Mater.* **1999**, *11*, 1214–1218.
(18) Gurunathan, K.; Murugan, A. V.; Marimuthu, R. M., U. P.; Amalnerkar, D. P. *Mater. Chem. Phys.* **1999**, *61*, 173–191.
(19) Mastragostino, M.; Arbizzani, C.; Paraventi, R.; Zanelli, A. *J. Electrochem. Soc.* **2000**, *147*, 407–412.
(20) Prasad, K. R.; Munichandraiah, N. *Electrochem. Solid-State Lett.* **2002**, *5*, A271–A274.
(21) Arbizzani, C.; Mastragostino, M.; Meneghello, L. *Electrochim. Acta* **1996**, *41*, 21–26.
(22) Moon, D. K.; Padias, A. B.; Hall, H. K.; Huntoon, T.; Calvert, P. D. *Macromolecules* **1995**, *28*, 6205–6210.
(23) Laforgue, A.; Simin, P.; Sarrazin, C.; Fauvarque, J.-F. *J. Power Sources* **1999**, *80*, 142–148.
(24) Frackowiak, E.; Khomenko, V.; Jurewicz, K.; Lota, K.; Beguin, F. *J. Power Sources* **2006**, *153*, 413–418.
(25) Patra, S.; Munichandraiah, N. *J. Appl. Polym. Sci.* **2007**, *106*, 1160–1171.
(26) Wang, J.; Xu, Y.; Chen, X.; Du, X. *J. Power Sources* **2007**, *163*, 1120–1125.

(27) Gaupp, C. L.; Welsh, D. M.; Rauh, R. D.; Reynolds, J. R. *Chem. Mater.* **2002**, *14*, 3964–3970.
(28) Gaupp, C. L.; Zong, K.; Schottland, P.; Thompson, B. C.; Thomas, C. A.; Reynolds, J. R. *Macromolecules* **2000**, *33*, 1132–1133.
(29) Reeves, B. D.; Grenier, C. R. G.; Argun, A. A.; Cirpan, A.; McCarley, T. D.; Reynolds, J. R. *Macromolecules* **2004**, *37*, 7559–7569.
(30) Stenger-Smith, J. D.; Webber, C. K.; Anderson, N.; Chafin, A. P.; Zong, K.; Reynolds, J. R. *J. Electrochem. Soc.* **2002**, *149*, A973–A977.
(31) Sarac, A. S.; Gilsing, H.; Gencturk, A.; Schulz, B. *Prog. Org. Coat.* **2007**, *60*, 281–286.
(32) Stenger-Smith, J. D.; Guenthner, A.; Cash, J.; Irvin, J. A.; Irvin, D. J. *J. Electrochem. Soc.* **2010**, *157*, A298–A304.
(33) Prasad, K. R.; Munichandraiah, N. *J. Power Sources* **2002**, *112*, 443–451.
(34) Welsh, D. M.; Kumar, A.; Meijer, E. W.; Reynolds, J. R. *Adv. Mater.* **1999**, *11*, 1379–1382.
(35) Yata, S.; Hato, Y.; Sakurai, K.; Osaki, T.; Tanaka, K.; Yamabe, T. *Synth. Met.* **1987**, *18*, 645–648.
(36) Fusalba, F.; Gouerec, P.; Villers, D.; Belanger, D. *J. Electrochem. Soc.* **2001**, *148*, A1–A6.
(37) Laforgue, A. *J. Power Sources* **2011**, *196*, 559–564.
(38) Staiti, P.; Lufrano, F. *J. Electrochem. Soc.* **2005**, *152*, A617–A621.

AM1007744